RAPID COMMUNICATIONS

PHYSICAL REVIEW B VOLUME 48, NUMBER 8 15 AUGUST 1993-II

Characterizing hot-carrier transport in silicon heterostructures with the use of ballistic-electron-emission microscopy

L. D. Bell, S. J. Manion, M. H. Hecht, W. J. Kaiser, R. W. Fathauer, and A. M. Milliken
Center for Space Microelectronics Technology, Jet Propulsion Laboratory, California Institute of Technology, Pasadena, California 91109
(Received 20 April 1993)

High-energy (0.1–1 eV) measurements of ballistic carrier transport in semiconductors have been performed using a new ballistic-electron-emission microscopy (BEEM) technique. Hot-electron attenuation lengths for *p*-type Si have been determined by combining precise Si molecular-beam-epitaxy methods with BEEM. A striking anomaly has been observed in the comparison of the 293- and 77-K results.

Electronic structure and charge carrier transport are key characteristics which determine the properties of many important semiconductor devices. The carrier scattering rate, for example, determines the collection efficiency of photovoltaics, the multiplication in avalanche photodetectors, the transit time of electrons in heterojunction bipolar transistors, and the high-field breakdown point in transistors. Since direct experimental probes of subsurface semiconductor electronic structure have not previously been available, the most critical transport properties, including carrier scattering, are not understood in detail. Because of the difficulty of controllably injecting electrons over a wide energy range (10 meV–10 eV) with high-energy resolution, the electronic structure and the energy-dependent carrier transport function have not been measured previously. In addition, conventional characterization techniques average electronic structure and transport information over a large area of the sample; therefore, they are insensitive to potentially important spatial variations.

We report an approach based on precise molecular-beam-epitaxy (MBE) methods and a new ballistic-electron-emission microscopy (BEEM) technique.[1,2] MBE growth provides microscopic control over the thickness and doping of the layers. Additionally, BEEM, based on scanning tunneling microscopy[3] (STM), allows direct control of the energy of carriers injected into a multilayer semiconductor structure. BEEM also lends the nanometer-scale spatial resolution inherent in STM techniques.[4] This approach has been applied to investigate both electronic structure and ballistic electron transport in silicon-based heterostructures.

BEEM has been used primarily to investigate metal/semiconductor (M/S) systems, providing a direct local measurement of Schottky barrier height and electron transport efficiency across the M/S interface with nanometer-scale resolution.[1,5] In addition, BEEM has been used to probe scattering mechanisms in the metal and at the interface,[6,7] and BEEM investigations have yielded attenuation length measurements for ballistic electrons in Au and PtSi.[4,8] These earlier measurements were not, however, sensitive to transport in the semiconductor. The present experiment differs from BEEM investigations of Schottky systems in that the BEEM measurements are performed on metallized silicon *pn* junctions. The samples studied were *p*-type Si layers with thicknesses ranging from 200 to 1000 Å, grown on *n*-type substrates, and covered with thin Au overlayers. In such structures, ballistic electrons must traverse hundreds of angstroms of silicon before reaching the potential barrier maximum. Only carriers which overcome this barrier are collected; therefore, this study probes the scattering mechanisms in the semiconductor. In the fully depleted *p* layers the barrier height is affected by the pinning position at the M/S interface, the doping level, and the thickness of the *p* layer. However, the energy barrier in a *pn* junction that is not fully depleted is controlled solely by doping level and is insensitive to variations in the M/S interface. BEEM spectroscopy of *pn* junctions yields values for barrier height as a function of *p*-layer thickness, which can be compared to calculated values. Moreover, comparison of the BEEM spectral shape for the *pn* junction to that for the Schottky barrier yields information regarding the energy dependence of scattering in the semiconductor versus that dependence in the metal. By varying the *p*-layer thickness and measuring the transmission efficiency at the barrier maxima, an attenuation length can be determined for minority carriers in *p*-type Si. Finally, performing these measurements at room temperature and in a liquid-nitrogen environment probes the temperature dependence of both barrier height and scattering mechanisms in the semiconductor.

The boron-doped *p*-type Si layers ($N_a = 5\times10^{17}$ cm^{-3}) were grown on *n*-type Si(100) substrates ($n = 2\times10^{15}$ cm^{-3}), by MBE at 600 °C. Prior to growth, the *n*-doped substrates were spin-etched with a 20% HF and ethanol solution to remove native oxide and hydrogen terminate the remaining silicon surface.[9] Samples were grown with *p*-layer thicknesses of 200, 500, and 1000 Å. An *n*-type substrate (referred to as the "0-Å structure") with no epitaxial layer was also examined. After growth the wafers were removed from the MBE system and diced into 9×9 mm^2 squares. A sample was then etched with CF_4 in a reactive-ion etching system with a Si mask to remove the *p* layer around the edges, decreasing edge leakage of the diode. Next the sample was transferred to a nitrogen-purged glove box where it was spin-etched with a 10% HF and ethanol solution. The sample was then

0163-1829/93/48(8)/5712(4)/$06.00

transferred directly into a UHV metal deposition chamber and 75 Å of Au was evaporated through a shadow mask, forming a metallized region of approximately 0.1 cm^2. Finally the sample was transferred to a separate nitrogen-purged glove box and loaded onto the STM. The STM has been described previously.[10]

The barrier height measurement is acquired by bringing the Au STM tip within tunneling range of the Au base layer and ramping the tip voltage negatively with respect to the base. An energy band diagram illustrating the tip emitter, the metal base, and the *p*-type and *n*-type Si layers is given in Fig. 1. Electrons tunnel from the tip through the vacuum barrier and enter the metal. These hot carriers travel through the base and cross into the *p* layer if they have sufficient energy to surmount the Schottky barrier. Additionally, those electrons which have energy greater than the barrier buried within the *p* layer and a transverse momentum that falls within the critical range for acceptance will cross the potential maximum and will travel through the *n* layer to be collected at the backside contact. [2]

An illustration of the energies of the conduction-band barrier maximum for the various *p* layers as a function of distance from the M/S interface is presented in Fig. 2(a).[11] Since the tunnel distribution is peaked at the Fermi level of the tip, ramping the tip voltage with respect to the base yields a sharply defined current threshold at the height of the barrier maximum. Typical BEEM spectra for *p*-layer thicknesses of 0 and 1000 Å are presented in Fig. 2(b). Similar spectra were recorded for each of the remaining thicknesses at room temperature, and the experiment was repeated at 77 K.

The experimental spectra are compared to a theory which employs phase-space-limited interface transmission and simple vacuum tunneling.[2] The theoretical spectra were fit to the data by adjusting the barrier height V_b and a scale factor R. The scale factor controls transmission intensity. Thus the critical parameters for characterizing the electronic structure, V_b, and transport, R, are directly derived from the data. As shown in Fig. 2(b), the agreement between the theoretical and experimental spectral shapes is excellent for both the Au/Si and the Au/*p*/*n*-type Si systems. As noted previously, carrier transport in the Au/*p*/*n*-type Si structure requires transmission through both the M/S interface and through the depletion region. In contrast, transport in the simple Schottky Au/Si system only requires transmission through the M/S interface. The good agreement between BEEM theory and spectra for the metallized *pn* junction structure demonstrates the ideal behavior of this system and the applicability of BEEM techniques to probing its electronic structure.

The experimental dependence of the derived barrier maximum, V_b, on *p*-layer thickness is illustrated in Fig. 3 along with theoretical calculations. The curves were generated using a finite element algorithm, HETMOD,[11] which solves Poisson's equation using the measured doping level and known surface pinning position, along with bulk semiconductor values. The data agree with theory within 20 meV. In particular, the agreement of the data from the sample with a 1000-Å *p* layer, which is not fully depleted and therefore has an energy maximum which is only dependent on doping, illustrates the ability of BEEM to accurately measure a well-known subsurface electronic barrier. Excellent agreement is also obtained for sample thicknesses when the barrier maximum depends on doping and thickness of the layer. This implies that the potential structure has been modeled correctly. The upward movement of the barrier maximum at low tempera-

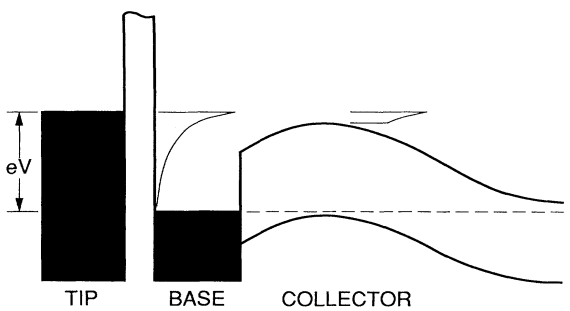

FIG. 1. Energy band diagram illustrating the Au STM tip, Au base region, and Si heterostructure collector. The critical transport region for electron collection is from the M/S interface to the barrier maximum in the *p* region.

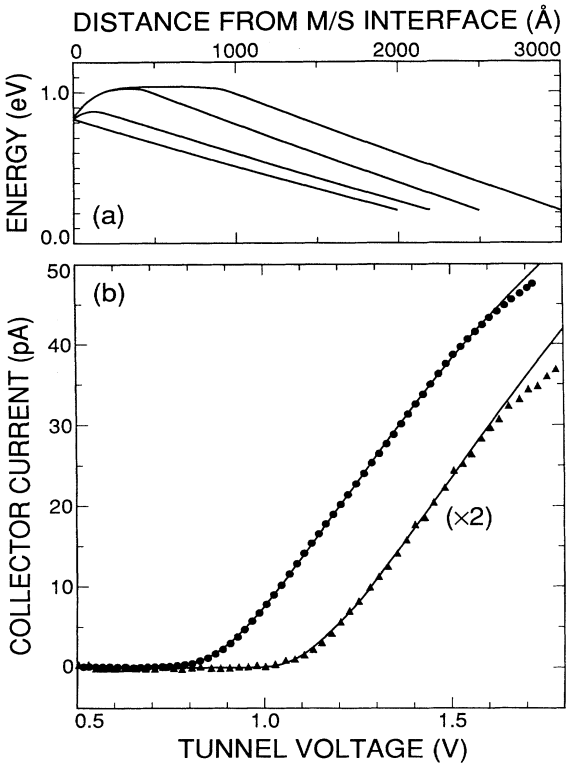

FIG. 2. (a) Potential profile for various *p*-layer thicknesses as a function of distance from the M/S interface. Note that the 1000-Å *p*-layer sample is not fully depleted. (b) BEEM spectra for Au/*n*-type Si system (circles) with $eV_b = 0.82$ eV and Au/*p*(1000 Å)-Si/*n*-type Si (triangles) with $eV_b = 1.04$ eV. The tunnel current for all spectra is 1 nA.

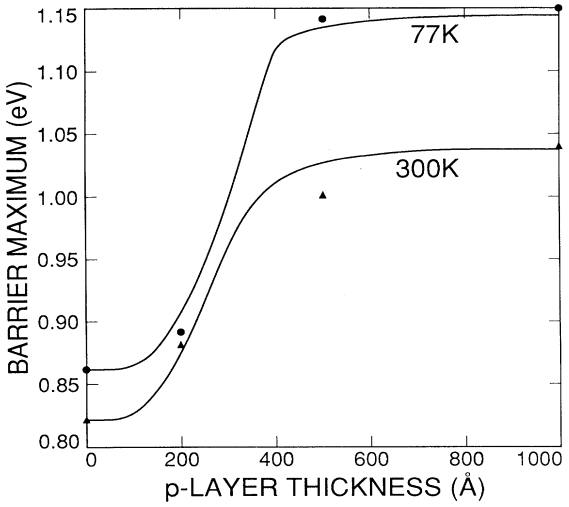

FIG. 3. Plot of barrier maximum as a function of p-layer thickness comparing BEEM measurements at 77 K (circles) and 300 K (triangles) to calculated values obtained from HETMOD.

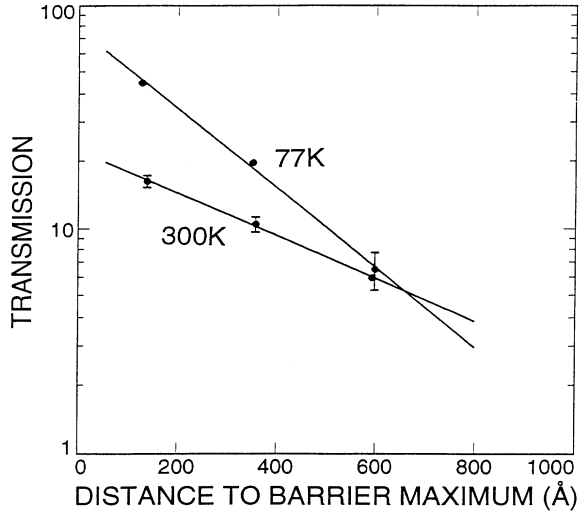

FIG. 4. Determination of attenuation length λ in Si pn samples at 300 and 77 K. $\lambda=240$ Å at 77 K and $\lambda=450$ Å at 300 K. Length of error bars represents two standard deviations, derived from all spectra taken for a given p-layer thickness and temperature. Error bars from the 200- and 400-Å, 77-K points and the 1000-Å, 300-K point are smaller than the plotted data point size.

ture is expected for all thicknesses, since the silicon band gap increases with decreasing temperature and the Fermi level moves toward the acceptor level.[12]

Knowledge of the distance to the barrier maximum in each sample allows for determination of the attenuation length in the p region. Hot electron propagation has a characteristic attenuation length λ, defined by the expression $I_c=I_0e^{-t/\lambda}$, where t is the distance from the M/S interface to the barrier maximum and I_c is the collector current. Therefore, by plotting the collection efficiency on a log scale as a function of the length of the region which must be traversed ballistically for collection, the attenuation length can be determined from the slope of the curve. It is important to note that λ, defined here as the attenuation length, is not a measure of the scattering length in the Si because of the three-dimensional nature of the scattering and the possibility of multiple scattering events. The attenuation length, as defined here, is experimentally unambiguous and is the quantity of significance for many device applications. The true mean free path is energy and momentum dependent and cannot be straightforwardly deduced from the attenuation length. Complete neglect of multiple scattering, for example, implies a mean free path approximately twice the attenuation length in an isotropic medium, as determined from an integration over all angles. The same attenuation length would be consistent with a much shorter mean free path in the presence of multiple scattering. The Monte Carlo approach described here was selected to allow for the more general case of scattering into states with different mean free paths. To measure collection efficiency, the scaling factor R was averaged for many different areas on a given sample. No correlation was found between R and the roughness of the Au metal overlayer. The resulting plot for attenuation length is presented in Fig. 4.

As illustrated in Fig. 2(b), the phase space model spectral shape is in good agreement with the shape of the metal-pn BEEM spectra. However, this model does not include scattering; therefore, it is not useful in predicting the attenuation length for hot electrons in p-type Si. In order to determine whether phonon emission accounts for the measured attenuation length, a Monte Carlo simulation was performed including phonon emission as the sole scattering process in the Si. This simulation was designed to estimate the attenuation length, as measured by BEEM, from the theoretical energy-dependent phonon emission rate. As a starting point, an energy-dependent mean free path was derived from the total phonon scattering rate as a function of energy.[13] In addition, a free-electron-like band was assumed with an effective mass of 0.98, corresponding to the longitudinal mass,[14] which is appropriate for propagation in the [100] direction. From these parameters a BEEM spectrum was generated and values of collector current at 0.5 V above threshold were used to calculate an attenuation length for this structure at zero temperature. It is appropriate to compare the 77-K experimental attenuation length with the zero-temperature calculation since the dominant scattering process is the emission of the 60-meV optical phonon. This theoretical model yielded an attenuation length of 150 Å which agrees well with the value of 240 Å measured at 77 K. However, the calculated spectral shape differs from that of the experimental curve when only this loss mechanism is included. This implies an energy dependence of the scattering processes differing from that included in the model or the presence of additional scattering mechanisms.

High-temperature (300 K) transport is sensitive to more complex processes including phonon absorption. The experimental results, shown in Fig. 4, yield a room-temperature attenuation length of 450 Å, longer than the 77-K results. This temperature dependence is opposite of that expected from traditional scattering models. The

presence of intervalley scattering may possibly explain this anomalous result. Since the four Si conduction-band minima at nonzero parallel momentum have small masses in the direction normal to the semiconductor layer, the mean free path in these minima will be longer in this direction. As a result of the increased scattering of electrons into these minima at higher temperatures, the measured attenuation length may be increased. In order to quantify this effect, further modeling is being performed.

In summary, these experimental results and their agreement with theory demonstrate the applicability of BEEM to the direct measurement of carrier transport in semiconductor structures. The precise control of the electronic structure of such systems, grown by MBE, provides an essential capability for transport analysis. This growth technique defines a subsurface barrier which can be effectively investigated by BEEM spectroscopy. In addition, BEEM allows direct control of injected carriers over a wide energy range, yielding accurate values for barrier height as a function of *p*-layer thickness in metallized *pn* junctions. In this experiment, we have demonstrated that BEEM can measure the barrier maximum in a *pn* junction within a 20-meV tolerance. BEEM spectroscopy of nondepleted samples, in which the barrier height is insensitive to variations in the M/S interface and is easily calculated, provide a check on the accuracy of BEEM theory. By varying the *p*-layer thickness and measuring the transmission efficiency at the barrier maxima, an attenuation length was determined for minority carriers in *p*-type Si. These experiments were performed at room temperature and at 77 K, probing the temperature dependence of barrier height and scattering mechanisms in silicon. Currently, similar studies of the electronic structure and electron transport are being performed on SiGe/Si-based heterostructures. The important capabilities described here may also be directed to the investigation of hole transport, carrier scattering, and electronic structure in a wide range of semiconductor structures.

The research described in this paper was jointly sponsored by the Office of Naval Research and the Strategic Defense Initiative Organization/Innovative Science and Technology Office through an agreement with the National Aeronautics and Space Administration. Useful discussions with Philipp Niedermann and Venkatesh Narayanamurti are gratefully acknowledged.

[1]W. J. Kaiser and L. D. Bell, Phys. Rev. Lett. **60**, 1406 (1988). For a more complete reference, see J. A. Stroscio and W. J. Kaiser, *Scanning Tunneling Microscopy* (Academic, San Diego, 1993), pp. 307–348.

[2]L. D. Bell and W. J. Kaiser, Phys. Rev. Lett **61**, 2368 (1988).

[3]G. Binning, H. Rohrer, Ch. Gerber, and E. Weibel, Phys Rev. Lett. **49**, 57 (1982).

[4]M. H. Hecht, L. D. Bell, W. J. Kaiser, and F. J. Grunthaner, Appl. Phys. Lett. **55**, 780 (1989).

[5]M. Prietsch and R. Ludeke, Phys. Rev. Lett. **66**, 2511 (1991).

[6]E. Y. Lee and L. J. Schowalter, Phys. Rev. B **45**, 6325 (1992).

[7]A. M. Milliken, S. J. Manion, W. J. Kaiser, L. D. Bell, and M. H. Hecht, Phys. Rev. B **46**, 12 826 (1992).

[8]Ph. Niedermann, L. Quattropani, K. Solt, A. D. Kent, and O. Fischer, J. Vac. Sci. Technol. B **10**, 580 (1992).

[9]P. J. Grunthaner, F. J. Grunthaner, R. W. Fathauer, T. L. Lin, M. H. Hecht, L. D. Bell, W. J. Kaiser, F. D. Schowengerdt, and J. H. Mazur, Thin Solid Films **183**, 197 (1989).

[10]W. K. Kaiser and R. C. Jaklevic, Rev. Sci. Instrum. **59**, 537 (1988).

[11]The data was fit using HETMOD—Heterostructure Modelling Program Version 1.7—written by Alan C. Warren of the Thomas J. Watson Research Center, Yorktown Heights, NY.

[12]S. M. Sze, *Physics of Semiconductor Devices*, 2nd ed. (Wiley, New York, 1981), pp. 15 and 27.

[13]J. Y. Tang and Karl Hess, J. Appl. Phys. **54**, 5139 (1983).

[14]S. M. Sze, *Physics of Semiconductor Devices* (Ref. 12), p. 850.